Aerospace Science and Technology 78 (2018) 559–568

Contents lists available at ScienceDirect

Aerospace Science and Technology

www.elsevier.com/locate/aescte

A variational approach for the dynamics of unsteady point vortices

Ahmed A. Hussein [a], Haithem E. Taha [b,*], Saad Ragab [c], Muhammad R. Hajj [c]

[a] Engineering Mechanics, Virginia Tech., 24061, USA
[b] Mechanical and Aerospace Engineering, University of California, Irvine, CA 92697, USA
[c] Engineering Mechanics, Virginia Polytechnic and State University, 495 Old Turner St, Blacksburg, VA 24061, USA

ARTICLE INFO

Article history:
Received 26 March 2018
Received in revised form 8 May 2018
Accepted 9 May 2018
Available online 15 May 2018

ABSTRACT

A Lagrangian formulation for the dynamics of unsteady point vortices is introduced and implemented. The proposed Lagrangian is related to previously constructed Lagrangian of point vortices via a gauge-symmetry in the case of vortices of constant strengths; i.e., they yield the exact same dynamics. However, a different dynamics is obtained in the case of unsteady point vortices. The resulting Euler–Lagrange equation derived from the principle of least action exactly matches the Brown–Michael evolution equation for unsteady point vortices, which was derived from a completely different point of view; based on conservation of linear momentum. The proposed Lagrangian allows for applying Galerkin techniques to the weak formulation of the vortex dynamics. The resulting dynamic model of time-varying vortices is applied to the problem of an impulsively started flat plate as well as an accelerating and pitching flat plate. In each case, the resulting lift coefficient using the dynamics of the proposed Lagrangian is compared to that using previously constructed Lagrangian, other models in literature, and experimental data.

1. Introduction

Reduced-order modeling of unsteady aerodynamics has been a topic of research interest since the early formulations of Prandtl [1] and Birnbaum [2]. These formulations were followed by the seminal works of Wagner [3] and Theodorsen [4]; the later efforts of Leishman [5,6] and Peters [7,8]; and in more recent papers by Ansari et al. [9,10], Taha et al. [11] and Yan et al. [12] among others. Because of its ability to account for deforming wakes associated with relatively large amplitude maneuvers, flexible wings, and arbitrary time-varying wing motions, development of the vortex lattice method (UVLM) [13–19] represents a hallmark in the history of unsteady aerodynamic modeling. In DVMs [20–22], a point vortex is released at each time step to satisfy the Kutta condition at the sharp edge it sheds from. Moreover, all of the shed vortices move with constant strengths that have been dictated at the shedding time by the Kutta condition. As such, Helmholtz conservation laws [23] dictate that the dynamics of these constant-strength point vortices will force them to convect with the fluid's local velocity, i.e. the Kirchhoff velocity, see Saffmann [24], pp. 10. Although DVMs were used to develop efficient numerical algorithms to solve for aerodynamic quantities associated with unsteady maneuvers, they require shedding point vortices at each time step, which increases the number of degrees of freedom considerably as the simulation time increases [25,26]. As a remedy, it has been suggested to replace the continuous shedding of constant-strength point vortices [27] with discontinuous/intermittent shedding of varying-strength point vortices, i.e. the strength of the most recent shed point vortex is adjusted each time step to satisfy the Kutta condition, instead of shedding a new vortex to achieve the same objective. Shedding is deactivated until the strength of the unsteady point vortex reaches an extremum [28]. At that instant, a new point vortex is shed from the same edge and the previous vortex is convected downstream with the Kirchhoff velocity while keeping its strength constant.

Variational principles have been shown to be useful physical-based approaches for deriving governing equations of both solids and fluids [29,30]. These equations are obtained by setting the first variation of the action, which is the time integral of a candidate Lagrangian function, to zero. Clebsh [29] and Hargreaves [31] derived the equations of motion for an inviscid, incompressible flow by defining the Lagrangian to be the integral of the fluid pressure. Later, Bateman [32] extended the principle to the case of compressible irrotational flow. Luke [33] showed that using variational principles, one is able to provide the boundary conditions by perturbing the limits of integration (Leibniz integral rule). Regarding the vortex motion, Bateman [32], followed by Serrin [34], showed that the equations of motion of vortex lines could be obtained from a variational approach with the ability to regularize

* Corresponding author.
E-mail address: hetaha@uci.edu (H.E. Taha).

https://doi.org/10.1016/j.ast.2018.05.010

Nomenclature

α	flat plate angle of attack	z_k	kth vortex position in Z plane $(x+iy)$
c	flat plate chord	ζ_k	kth vortex position in ζ plane $(\xi+i\eta)$
F_x, F_y	flat plate forces in x and y directions respectively	$\zeta_k^{(I)}$	Image position of kth vortex in ζ plane $(\xi+i\eta)$
Γ_k	kth vortex strength	$\lvert\ \rvert$	Absolute value of complex number, $\lvert z\rvert=\sqrt{x^2+y^2}$
w_k	regularized fluid velocity of kth vortex	$\dot{(\,)}$	derivative w.r.t. time
$W, \tilde{W}$	Kirchhoff–Routh functions in flat plate and circle plane respectively	$(\,)^*$	conjugate
z_c	flat plate centroid position in Z plane	$(\,)'$	derivative w.r.t. ζ, $\frac{d}{d\zeta}$

the infinite velocity at the vortex center (Sec. 4 in Ref. [32]). These variational principles were also used to derive governing equations for the cases of fluid motion with distributed vorticity [35] or point vortices [36] with no boundaries, and for the case of a fluid-body interaction [37] that considered constant strength vortices only. Advances made in studying the Hamiltonian dynamics of point vortices [38,36,39] point to the potential of developing a variational principle governing the dynamics of unsteady point vortices interacting with a circular cylinder or a body conformal to it (e.g., airfoil), which is the objective of this work. Such a formulation will allow satisfaction of conservation laws via adding constraints to the variational problem. In addition, it will enable compact and efficient coupling with other variational principles governing rigid body and structural dynamics for coupled unsteady flight dynamics analysis and/or aeroelastic analysis. To date, there have been no developments for variational principles governing the dynamics of unsteady point vortices interacting with solid bodies enclosed by a non-zero total circulation.

The dynamics of constant-strength, point vortices in an inviscid fluid, which is governed by the Biot–Savart law, was derived by Chapman [38] from an action whose Lagrangian is the summation of two functions. The first function is a bilinear function in the vortex spatial coordinates and its velocity, and the second one is the Routh stream function. Recently, Shashikanth et al. [39] proved that the equations of motion for a cylinder moving in the presence of constant-strength vortices of zero sum (i.e., zero total circulation), known as Foppl problem [40,41], have a Hamiltonian structure. Dritschel and Boatto [42] showed similar results for three dimensional differentiable surfaces conformal to a sphere.

In the present work, we present a new Lagrangian function for the dynamics of point vortices that is more general than Chapman's [38]. We examined the relation between the proposed Lagrangian and Chapman's Lagrangian for the cases of constant strength and time-varying point vortices. Interestingly, the proposed Lagrangian dynamics of unsteady point vortices recovers the momentum based Brown–Michael model [43]. We applied the Galerkin technique to the resulting weak formulation of the time-varying vortices for the problem of an impulsively started flat plate as well as an accelerating and pitching flat plate, with comparison to experimental data in the literature [44,45]. To the best of our knowledge, this is the first variational principle to govern the dynamics of unsteady point vortices.

2. Lagrangian dynamics of point vortices

2.1. General formulation

Considering the flow around a sharp-edged body (in the z-plane) and mapping it to the flow over a cylinder (in the ζ-plane) with an interrelating conformal mapping $z=z(\zeta)$, as shown in Fig. 1, the regularized local fluid velocity (Kirchhoff velocity) of the shed kth vortex is given by [46–48]

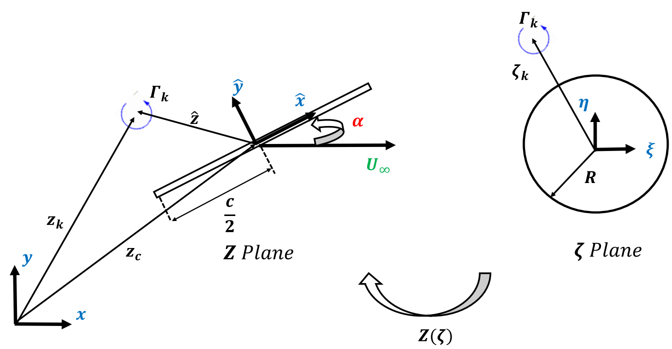

Fig. 1. Conformal mapping between a sharp-edged body and a circular cylinder.

$$\frac{dz_k}{dt}=w_k(z_k)=\frac{1}{[z'(\zeta_k)]^*}\lim_{\zeta\longrightarrow\zeta_k}\left[\frac{\partial F}{\partial\zeta}-\frac{\Gamma_k}{2\pi i}\frac{1}{\zeta-\zeta_k}-\frac{\Gamma_k}{4\pi i}\frac{z''(\zeta)}{z'(\zeta)}\right]^* \tag{1}$$

where F is the complex potential, Γ_k is the strength of the kth vortex, and the asterisk refers to a complex conjugate. The last term on the right hand side, which involves the second derivative of the transformation, was first derived by Routh then by Lin [46] and later by Clements [47].

Lin [49] showed the existence of a Kirchhoff–Routh function W (Ref. [50] sec. 13.48) that relates the velocity components of the kth vortex to the derivatives of W, in a Hamiltonian form such that the velocity components of the vortex in z plane are

$$\Gamma_k u_k=\frac{\partial W}{\partial y_k},\qquad \Gamma_k v_k=-\frac{\partial W}{\partial x_k} \tag{2}$$

The Kirchhoff–Routh function $\tilde{W}$ in the circle plane is related to the stream function ψ_0 by [46,50,51]

$$\tilde{W}(\xi_k,\eta_k)=\Gamma_k\psi_o(\xi_k,\eta_k)+\sum_{k,l,k\neq l}\frac{\Gamma_k\Gamma_l}{4\pi}\left[\ln|\zeta_k-\zeta_l|-\ln|\zeta_k-\zeta_l^I|\right]+\sum_k\frac{\Gamma_k^2}{4\pi}\ln|\zeta_k-\zeta_k^{(I)}| \tag{3}$$

where ψ_o is the stream function of the body motion (i.e., $F=F_0+\sum_{k=1}^n\Gamma_k$ and $F_0=\phi_0+i\psi_0$). Then the relation between the Kirchhoff–Routh function W in the flat plate plane and that in circle plane $\tilde{W}$ is given as [46]:

$$W=\tilde{W}+\sum_k\frac{\Gamma_k^2}{4\pi}\ln|\frac{dz}{d\zeta}| \tag{4}$$

It is noteworthy that, as shown by Lin [49], the term ρW is a measure of the kinetic energy, where ρ is the density of the fluid. As such, the equations of motion can be determined from an energy minimization process. More details about the Hamiltonian structure of the motion of point vortices are provided by Aref [52].

2.2. Proposed Lagrangian of point vortices

We postulate a new Lagrangian function for the motion of point vortices in an infinite fluid in the z-plane in the most basic form as

$$L(z_k, z_k^*, \dot{z}_k, \dot{z}_k^*) = \frac{1}{i}\sum_{k=1}^{n}\Gamma_k z_k^* \dot{z}_k + W \tag{5}$$

where the first term is the bilinear function in variables z_k and $\dot{z}_k$, and the second term is the Routh stream function

$$W = -\frac{1}{2\pi}\sum_{k,l,k\neq l}\Gamma_k\Gamma_l \ln(z_k - z_l)(z_k - z_l)^* \tag{6}$$

It has to be pointed out that the variable z_k and its conjugate z_k^* are treated as an independent variables. The bilinear nature of the first term ensures that the resulting equations of motion will involve only time derivatives of the first order. The same concept was introduced by Chapman whose Lagrangian is written as

$$\begin{aligned} L'(z_k, z_k^*, \dot{z}_k, \dot{z}_k^*) &= \frac{1}{2i}\sum_{k=1}^{n}\Gamma_k(z_k^*\dot{z}_k - z_k\dot{z}_k^*) \\ &\quad - \frac{1}{2\pi}\sum_{k,l,k\neq l}\Gamma_k\Gamma_l \ln(z_k - z_l)(z_k - z_l)^* \\ &= I_0 + W \end{aligned} \tag{7}$$

where I_0 is one of the constants of motion associated with the motion of vortices of constant strengths in an infinite fluid. This Lagragian was then used in different contexts [53,54].

It is interesting to note that the proposed Lagrangian L and Chapman's Lagrangian L' are related via a gauge symmetry for the case of constant-strength vortices. That is, we have

$$L' = L - \frac{1}{2i}\frac{d}{dt}\sum_{k=1}^{n}\Theta_k \tag{8}$$

where $\Theta_k = \Gamma_k z_k^* z_k$ is the angular momentum of the kth vortex about the origin. Note that the gauge symmetry between any two Lagrangian functions such as L and L' implies that they add up to a total time derivative of some function, i.e., we have

$$L' = L + \frac{d}{dt}[F(q,t)] \tag{9}$$

where q are the generalized coordinates. As such, it is said that L and L' are related by a gauge symmetry or a gauge transformation and that both are gauge invariant [55,56].

On the other hand, using Eq. (8), one may explain Chapman's Lagrangian L' as a constrained version of our proposed Lagrangian L to satisfy the constraint that the total angular momentum of the vortices about origin is conserved; i.e., $\frac{d}{dt}\sum_{k=1}^{n}\Theta_k = 0$.

2.3. Dynamics of a constant strength point vortices

To obtain the equations of motion for the case of vortices of constant strength, we define the action to be the integral of the Lagrangian

$$S = \int_{t_1}^{t_2} L(z_k, z_k^*, \dot{z}_k, \dot{z}_k^*)dt \tag{10}$$

Applying the principle of least action, i.e., setting the first variation of the action integral S to zero, the corresponding Euler–Lagrange equations are written as

$$\frac{d}{dt}\left(\frac{\partial L}{\partial \dot{z}_k}\right) - \frac{\partial L}{\partial z_k} = 0 \tag{11}$$

which yields the Biot–Savart law [57,50,19] that governs the motion of point vortices and is given by

$$\dot{z}_k^* = \frac{1}{2\pi i}\sum_{k,l,k\neq l}\frac{\Gamma_j}{z_k - z_l} \tag{12}$$

It should be noted that the same result can be obtained using Chapman's Lagrangian L' [38].

2.4. Dynamics of unsteady point vortices interacting with a conformal body

For a single point vortex of constant strength Γ, the Lagrangian proposed in Eq. (5) is written as

$$L(z, z^*, \dot{z}, \dot{z}^*) = \frac{1}{i}\Gamma z^* \dot{z} + W(z, z^*) \tag{13}$$

where $W(z, z^*)$ is the Kirchhoff–Routh function, which is a measure of the instantaneous energy in the flow [49] while accounting for the presence of the body. Allowing for a time-varying vortex strength (i.e. $\Gamma = \Gamma(t)$), a term that depends on the time rate of change of circulation (i.e. $\dot{\Gamma}$)) is added to ensure that the derivatives resulting from the bilinear function are coordinate-independent [38,53,54]. As such, the Lagrangian is written as

$$L(z, z^*, \dot{z}, \dot{z}^*) = \frac{1}{i}\left(\Gamma z^*\dot{z} + \dot{\Gamma} z_0^* z\right) + W(z, z^*) \tag{14}$$

where z_0 is the coordinate of an arbitrary point on the body.

Now the Lagrangian of n point vortices of time-varying strengths is written as

$$L(z_k, z_k^*, \dot{z}_k, \dot{z_k}^*) = \frac{1}{i}\sum_{k=1}^{n}\left(\Gamma_k z_k^*\dot{z}_k + \dot{\Gamma} z_{0k}^* z_k\right) + W(z_k, z_k^*) \tag{15}$$

where z_{0k} is the coordinate of a reference point on the body, which is usually the coordinate of the edge from which the vortex is shed [43,58,59,48].

Applying Euler–Lagrange equations (11) associated with minimizing the action integral based on this transformed Lagrangian (15), we obtain the dynamics of an unsteady point vortex as

$$\dot{z}_k + \frac{\dot{\Gamma}_k}{\Gamma_k}(z_k - z_{0k}) = \left(\frac{i}{\Gamma_k}\frac{\partial W}{\partial z_k}\right)^* \tag{16}$$

which reduces to the Biot–Savart law given by Eq. (12) if $\dot{\Gamma}$ is set to zero.

The right hand side of Eq. (16) can be represented in terms of the regularized local fluid velocity (Kirchoff velocity) $w^*(z_k)$, obtained from Eq. (1) as shown by [50], which is expressed as

$$\left(\frac{i}{\Gamma_k}\frac{\partial W}{\partial z_k}\right)^* = w^*(z_k) \tag{17}$$

Combining Eq. (16) and Eq. (17), we write

$$\dot{z}_k + \frac{\dot{\Gamma}_k}{\Gamma_k}(z_k - z_{0k}) = w^*(z_k) \tag{18}$$

which is exactly the same equation obtained by Brown and Michael [43] from a completely different approach that was based on a linear momentum argument.

It is interesting to note that while both the proposed Lagrangian L and Chapman's L' [38] yield the exact same dynamics, i.e. the Biot–Savart law for constant-strength vortices, they yield different dynamics for unsteady point vortices. Adding the same term introduced in Eq. (15) to Chapman's Lagrangian L' to obtain a coordinate-independent expression for the vortex absolute velocity,

$$L'(z_k, z^*, \dot{z}_k, \dot{z}_k^*) = \frac{1}{2i}\sum_{k=1}^{n}\left(\Gamma_k(z_k^*\dot{z}_k - z_k\dot{z}_k^*) + \dot{\Gamma} z_{0k}^* z_k\right) + W(z_k, z_k^*) \tag{19}$$

minimizing the action integral based on this transformed Lagrangian (19), the resulting equation of motion is

$$\dot{z}_k + \frac{\dot{\Gamma}_k}{2\Gamma_k}(z_k - z_{0k}) = w^*(z_k) \tag{20}$$

which differs from that of Brown–Michael by the factor of one half that multiplies the $\dot{\Gamma}$-term.

Next, we apply the variational principle approach as defined above and evaluate the performance of both postulated and Chapman's [38] Lagrangians in predicting flow quantities. Particularly, we compare time histories of the circulation and lift coefficient to those obtained using the impulse matching model by Wang and Eldredge [48] and Wagner's function [3].

3. Numerical results

The equations of motion, and the forces acting on an impulsively started flat plat are derived in Appendix A. Three types of airfoil motion are considered in this section: (i) an impulsively started motion in which the airfoil is suddenly accelerated to velocity U_∞, (ii) a finite acceleration from rest to reach U_∞ after some non-zero but finite time, and (iii) and the vortex generated by a pitching plate. The weak for of Eq. (16) is written as

$$\delta S = 0 \tag{21}$$

The weak form is then integrated using one of the Galerkin techniques defined in Ref. [60]. The weak-formulation-based finite element solution can not be applied to Eq. (16) of Brown and Michael because it is in a strong form, and reducing it to a weak form is not direct. The enabling of this capability is one of the main contributions of this effort.

3.1. Impulsively started flat plate

First, similar to the classical unsteady thin airfoil theory (e.g., Wagner [3], Theodorsen [4], and Von Karman and Sears [61]), we assume that the starting vortex moves along the x-axis and the local fluid velocity is U_∞ (i.e., $w(z_v) = U_\infty$). As such, the evolution equation (A.5) in the z planes is written as

$$\dot{x}_v + \frac{\dot{\Gamma}_v}{\beta\Gamma_v}(x_v - x_{v0}) = U_\infty \tag{22}$$

where β is a factor that results from the Lagrangian used in deriving the equation of motion. $\beta = 1$ for the proposed Lagrangian and $\beta = 2$ for Chapman's Lagrangian.

The evolution equation of the impulse matching model [59,48] can also be simplified to

$$\dot{x}_v + \frac{\dot{\Gamma}_v}{\Gamma_v}\frac{(x_v^2 - x_{v0}^2)}{x_v} = U_\infty \tag{23}$$

Fig. 2 shows the time variations of the normalized vortex strength Γ, the lift coefficient C_L, and the time-variation of the normalized vortex location x for the case of $\alpha = 5°$. Plots from simulations based on (i) the proposed Lagrangian dynamics ($\beta = 1$ Brown–Michael), (ii) Chapman's Lagrangian ($\beta = 2$), (iii) the impulse matching model of Wang and Eldredge [48], and (iv) Wagner's [3] step response function are presented for the sake of comparison. The plots show that all models agree qualitatively with Wagner's exact potential flow solution. Note that in the three models, the infinite sheet of wake vorticity is approximated by a single vortex. As expected, the correction to the Kirchhoff velocity (taken as U_∞ here) in the case of $\beta = 2$ is half of that in the case of $\beta = 1$ yields slightly higher (spurious) lift.

Next, we consider increasing the angle of attack to $\alpha = 10°$ to relax the flat wake assumption. Thus allowing the vortex to move in the plane, i.e. with two degrees of freedom. Fig. 3 shows the resulting time variations of the normalized circulation Γ, lift coefficient C_L, vortex position along the x-axis, and the slope of the vortex trajectory θ as a function of x. The singular value of the lift at $t = 0$, which corresponds to the added mass effect, is removed to highlight the difference between results from different models. Again, the results based on L' ($\beta = 2$) predict a larger vortex strength (airfoil circulation) and a slightly higher lift, than those predicted by the two other models. Fig. 3d shows that the slope of the starting vortex asymptotically approaches a line parallel to the incident free stream (i.e. $\theta \approx \alpha = 10°$). As shown, the proposed Lagrangian (Brown–Michael model) yield lift and circulation values that do no match Wagner's function. In addition, the impulse matching results in a slower downstream convection. Consequently the development of circulation takes place at a slower rate with an overall effect of reduced lift coefficient that matches Wagner's function. We note, however, that the Wagner's response should not be considered as a reference for comparison in this case because of the flat-wake and shedding by U_∞ assumptions that may not be appropriate for the relatively large angle of attack. This can be seen from the high-fidelity results in Fig. 3b as the lift starts to disagree with Wagner's function after non-dimensional time of $U_\infty t/c > 1.2$. The high-fidelity results was produced in Ref. [48] using the viscous vortex particle method developed by Eldredge [62].

3.2. Flat plate accelerating from rest

Next, we consider the lift on a flat plate that accelerates from rest. To validate our results, we consider the velocity profile of Beckwith and Babinsky [44] that is shown in Fig. 4. In that experiment, the airfoil is accelerated to the velocity $U_\infty = 0.48$ m/s over a distance of 0.6 chords.

The velocity profile of the accelerated flat plate, shown in Fig. 4a, is obtained from the data of Beckwith and Babinsky [44] via the following optimization problem

$$\min_{P_m} \sum_{i=1}^{N}\left(X_i - \sum_{0}^{m}(P_m t^m)\right) \tag{24}$$

subject to the end constraints

$$\dot{X}_P(0) = 0,\ \ \dot{X}_P(t_f) = U_\infty,\ \text{ and }\ \ddot{X}_P(t_f) = 0 \tag{25}$$

where $X_P = \sum_0^m P_m t^m$ represents the polynomial fit to the given data, N is the number of sample points ($X_i's$) taken from Fig. 4b in Ref. [44] by Beckwith and Babinsky, and m is the degree of the fitting polynomial. We used the **fmincon** Matlab function for solving

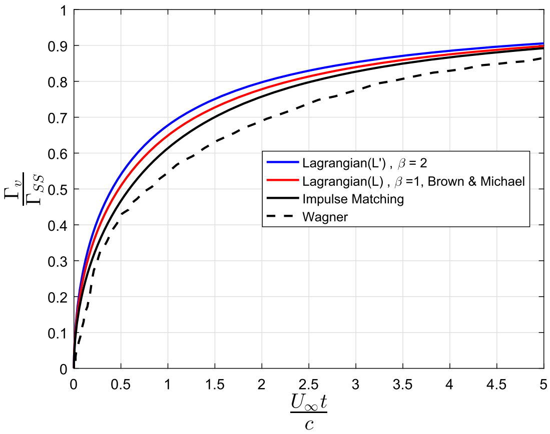

(a) Time variation of the normalized vortex strength Γ_v. The circulation is normalized with the steady-state value Γ_{SS}.

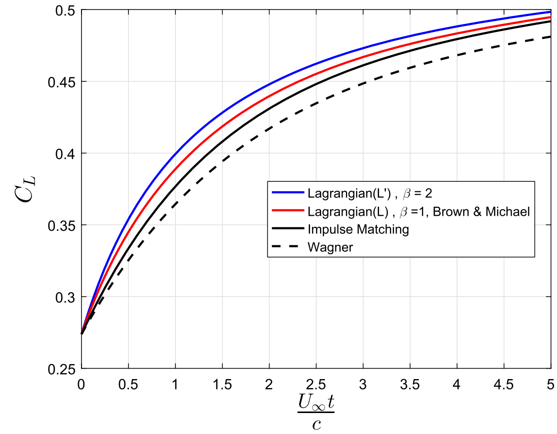

(b) Time variation of the lift coefficient C_L

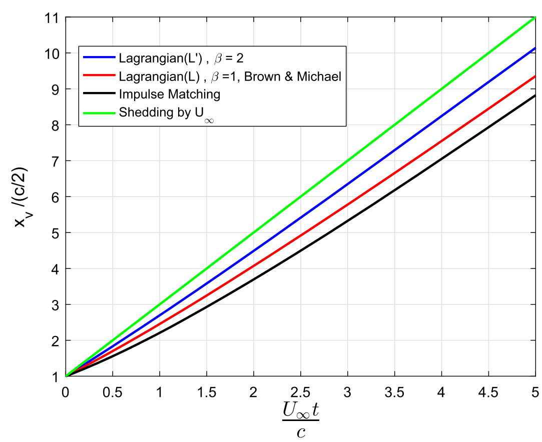

(c) Time variation of the normalized vortex position x_v. The position is normalized using the semi-chord of the airfoil.

Fig. 2. Time variations of (a) the normalized circulation, (b) lift coefficient and (c) normalized position of the starting vortex for $\alpha = 5°$ and the vortex is assumed to move only in the x direction. The time is normalized using the airfoil speed U_∞ and chord c. (For interpretation of the colors in the figure(s), the reader is referred to the web version of this article.)

the constrained optimization problem defined above. The resulting equation for the commanded and the measured positions respectively are

$$X_C(t) = -8.7540t^4 + 5.3376t^3 - 0.0265t^2 + 0.004$$
$$X_M(t) = -8.3073t^4 + 5.0119t^3 + 0.0233t^2 - 0.0002t + 0.004 \quad (26)$$

Because few number of "measured data" points were available for fitting, we present results for both maneuvers; commanded and measured. In addition, we use the extended lifting line theory [63] to account for three-dimensional effects on the lift which implies a correction factor of 0.618 based on aspect ratio $Æ = 4$.

Fig. 5 shows time variations of the normalized circulation and lift coefficient for a flat plate accelerating from rest using both commanded and measured fits of the velocity profile. The plots show agreement among all representations except that the predicted circulation and lift based on Chapman's Lagrangian [38] is slightly higher and show faster convergence to the steady state value. The lift coefficient shows that the proposed Lagrangian (Brown–Michael equation) yields values that are closer to the experimental data of Beckwith and Babinsky [44] than both Chapman's Lagrangian ($\beta = 2$) and the impulse matching model of Wang and Eldredge [48], particularly in capturing the transient peak. The large overshoot in the lift coefficient for $\beta = 2$ indicates that the exclusion of the symmetry term (angular momentum constraint) is necessary to satisfy the linear momentum around the vortex and the branch cut in an integral sense. In other words, the evolution equation based on the Lagrangian L' violates the conservation of linear momentum around the vortex and the shedding edge. Hence, the proposed Lagrangian L is a more general (unconstrained) Lagrangian of point vortices. It governs the dynamics of both vortices of constant and time-varying strengths.

3.3. Pitching flat plate

In Fig. 6, the lift coefficient versus angle of attack is shown for an airfoil pitching at a reduced frequency $k = 0.2$ ($k = \dot{\alpha}_{max}c/(2U_\infty)$), and compared to the experiment carried out by Granlund et al. [45] at Reynolds number $Re = 20{,}000$. We followed the pitching kinematics defined by Eldredge in Ref. [64] as

$$\alpha(t) = \alpha_{max}\frac{G(t)}{max(G(t))} \quad (27)$$

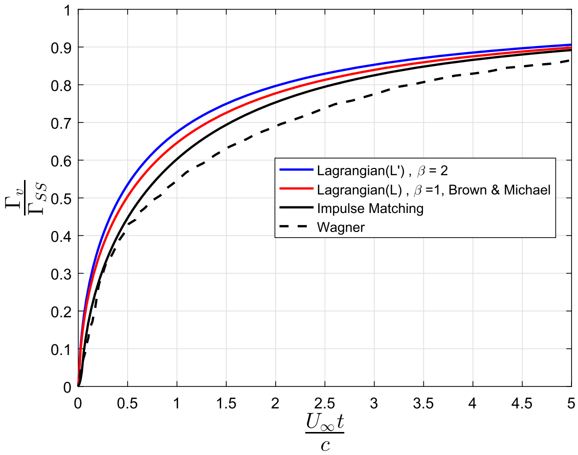

(a) Time variation of the normalized vortex strength Γ_v. The circulation is normalized with the steady-state value Γ_{SS}

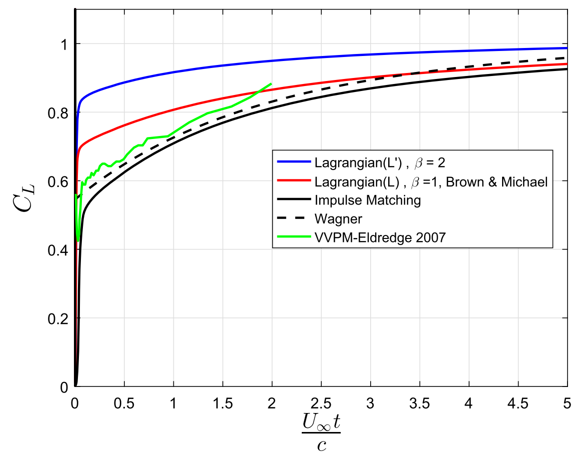

(b) Time variation of the lift coefficient C_L

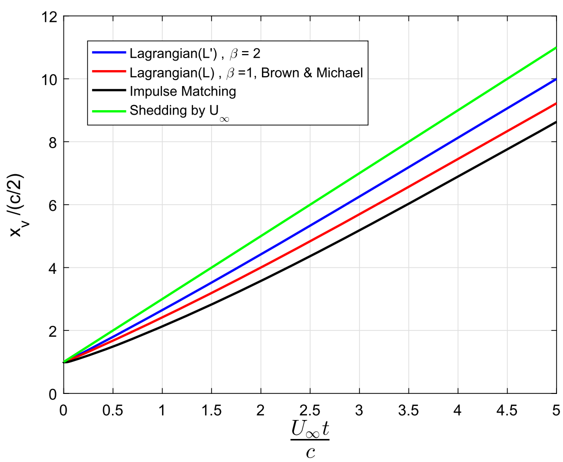

(c) Vortex position x_v versus non-dimensional time

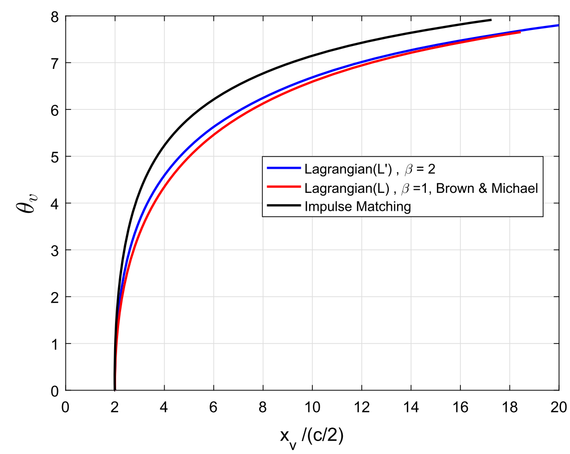

(d) Slope of the vortex trajectory θ_v versus vortex position x_v

Fig. 3. Time variations of (a) the normalized circulation, (b) lift coefficient, (c) normalized position of the starting vortex, and the slope of the vortex trajectory for $\alpha = 10°$ and the vortex is allowed to move freely in the plane of the airfoil. The time is normalized using the airfoil speed U_∞ and chord c.

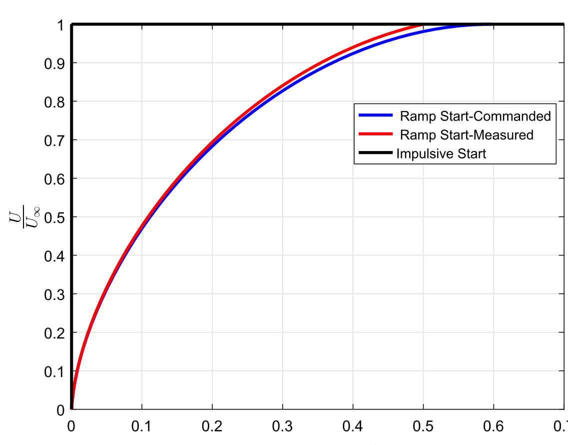

(a) Velocity profiles for the accelerated airfoil-Beckwith and Babinsky[45]

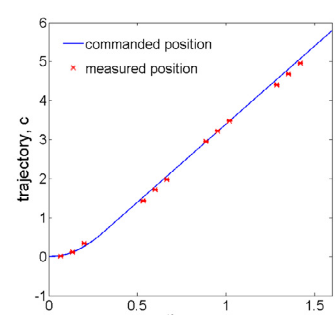

(b) Commanded and actual trajectory profile for the airofoil motion-Beckwith and Babinsky [45]

Fig. 4. Kinematics for the accelerated flat plate.

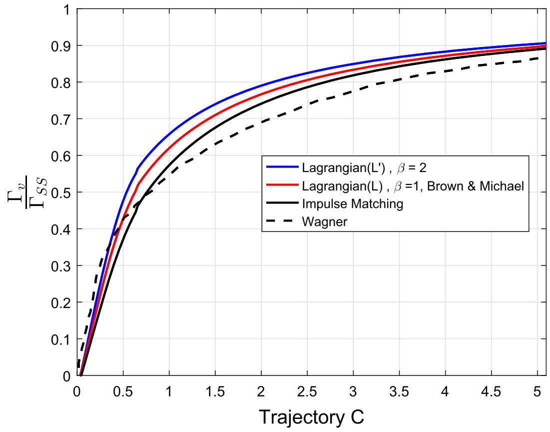

(a) Time variation of the normalized vortex strength Γ_v for the *commanded* position. The circulation is normalized with the steady-state value Γ_{SS}

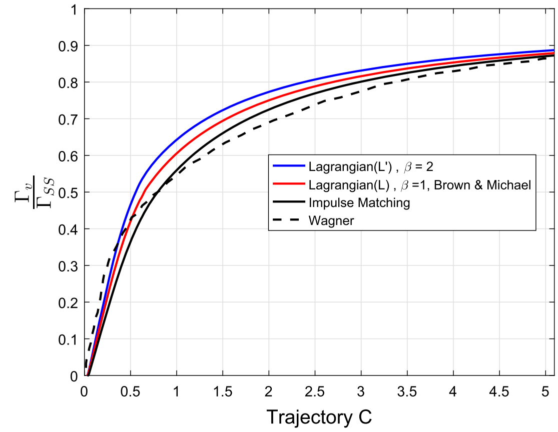

(b) Time variation of the normalized vortex strength Γ_v for the *measured* position. The circulation is normalized with the steady-state value Γ_{SS}

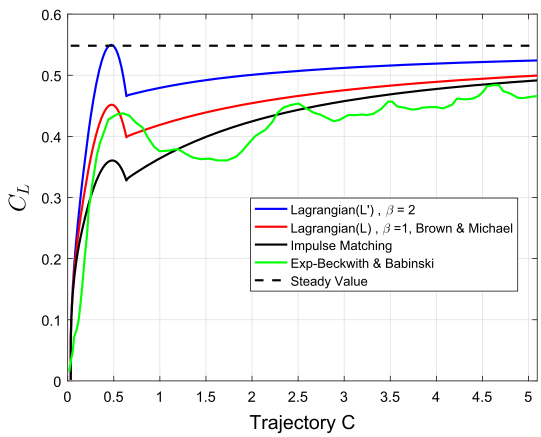

(c) Time variation of the normalized lift coefficient C_L for the *commanded* position

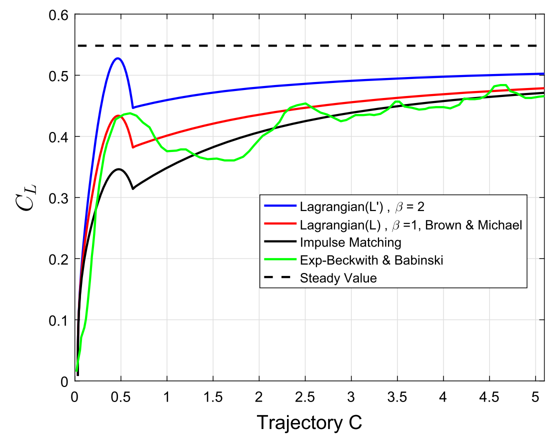

(d) Time variation of the normalized lift coefficient C_Le for the *measured* position

Fig. 5. Time variations of the normalized circulation and lift coefficient for $\alpha = 5°$ for the accelerated flat plate.

where $G(t)$ is defined as

$$G(t) = \ln\left(\frac{\cosh(aU_\infty(t - t_1)/c)\cosh(aU_\infty(t - t_3)/c)}{\cosh(aU_\infty(t - t_2/c)\cosh(aU_\infty(t - t_4)/c)}\right) \tag{28}$$

In this case, two vortices are shed from the leading and trailing edges. The same trend as in the case of the starting vortex is noted. Moreover, the difference is maximum when the angle of attack reaches 45° and approaches zero when the angle of attack reaches 90°. We also noted that while both proposed and Chapman's Lagrangian yielded similar dynamics for the case of the starting vortex, they yielded different dynamics for the case of pitching flat plate. Although the proposed Lagrangian (Brown–Michael) yielded a better agreement with the experimental results than Chapman's Lagrangian, the Impulse matching results have a better agreement with the experimental unlike the accelerating flat plate problem.

It should be pointed out that the present work is not favoring Brown–Michael model over Eldredge's impulse matching model or vice versa. The main outcome of this work is to provide a variational formulation for the dynamics of unsteady point vortices, which interestingly matches the momentum-based formulation of Brown and Michael. However, as pointed out by Wang and Eldredge [48] that either model is not alone sufficient for developing reduced-order models of two-dimensional unsteady aerodynamics. The Brown–Michael model (equivalently its present variational version) or the impulse matching model represents only one part

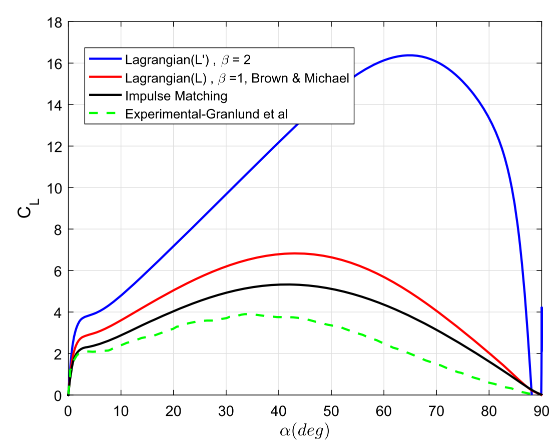

Fig. 6. Lift coefficient versus angle of attack for pitching airfoil at reduced frequency $k = 0.2$ and Reynolds number $Re = 20{,}000$.

in the whole formulation which also includes a shedding criterion and an auxiliary condition (Kutta-like condition). It should be noted that the comparison between the lift histories from the Brown–Michael [43] and the impulse matching [48] models may not reveal which model capture the true vortex dynamics. Both lift time histories shown in Fig. 6 are obtained by applying the Kutta condition which may not be applicable in this high angle of attack unsteady flow. To reflect more on the issues discussed in this paper, the authors will cover in their future work other kinematics problems such as perching and plunging motions, and will verify them against experimental data [45,65,66].

4. Potential and future advancements

The main contribution of this effort is providing a successful Lagrangian function that governs the dynamics of unsteady point vortices. Having this Lagrangian invokes the development of variational principles that govern flight dynamics and/or aero-elastic systems. There have been several successful variational principles governing structure dynamics (e.g., the principle of minimum potential energy). The dynamics of the aeroelastic system is typically written as

$$\frac{d}{dt}\left(\frac{L_s}{\partial \dot{q}_s}\right) - \frac{\partial L_s}{\partial q_s} = Q \tag{29}$$

where q_s are the structural generalized coordinates, L_s is the Lagrangian function of the structural system, and Q represents the non-conservative applied loads. In this typical formulation, the aerodynamic loads (of unknown nature) are incorporated in the right hand side as non-conservative loads; due to the lack of an *aerodynamic* Lagrangian and/or variational principle for unsteady fluids even within the framework of potential flow.

Using the proposed Lagrangian L for unsteady aerodynamics, we can, for the first time, write a *single* Lagrangian L_{tot} governing the dynamics of the whole aero-elastic system; providing a single variational principle for both the fluid flow and structure, which has been the subject of interest for decades [67]. As such, the aerodynamic loads will be naturally accounted for in a similar fashion to the structural restoring forces in the left hand side of Lagrange's equations

$$\frac{d}{dt}\left(\frac{L_{tot}}{\partial \dot{q}}\right) - \frac{\partial L_{tot}}{\partial q} = 0 \tag{30}$$

where $q = [q_s \, q_a]$ and q_a represents the generalized coordinates of the aerodynamic system (e.g., position and strength of the shed vortices). The variational equation (30) will invoke discovery of conserved quantities and more compact analysis of aeroelastic systems.

5. Conclusions

We investigated the potential of implementing variational principles to derive governing equations for the interaction of unsteady point vortices with a solid boundary. To do so, we postulated a new Lagrangian function for the dynamics of point vortices that is more general than Chapman's. We showed that this function is related to Chapman's Lagrangian via a gauge symmetry for the case of constant-strength vortices. In other words, both Lagrangian functions result in the same governing equation, i.e. the Biot–Savart law is directly recovered from the Euler–Lagrange equations corresponding to minimization of the action integral with these two Lagrangians. We also found that, unlike Chapman's Lagrangian, the principle of least action based on the proposed Lagrangian results exactly in the Brown–Michael model for the dynamics of unsteady point vortices. We implemented the resulting weak formulation of the time-varying vortices to the problem of an impulsively started flat as well as an accelerating and pitching flat plate. The weak form is then integrated using Galerkin technique for finite element. For the case of accelerating flat plate, the resulting time history of the lift coefficient from the three models (variational approach based the proposed Lagrangian and Chapmann's and the impulse matching model) is compared against the experimental results of Beckwith and Babinsky. The results showed a better agreement for the variation approach using the proposed Lagrangian. On the other hand, the results of the impulse matching model for the pitching flat plat agree better with experimental results than the those based on Chapmann's and the proposed Lagrangian (Brown–Michael model).

Conflict of interest statement

There is no conflict of interest in this work.

Acknowledgements

The authors acknowledge the support of the NSF Grant CMMI-1435484. We would like to thank Dr. Babinsky for kind cooperation in explaining the experimental results and for providing the data shown in Fig. 4b.

Appendix A. Impulsively stared flat plate (the starting vortex problem)

We consider a flat plate of semi-chord $c/2$ mapped from a circle of radius R, as shown in Fig. 1, according to the conformal mapping

$$z_v(\zeta_v) = z_c + g(\zeta_v)e^{i\alpha} \tag{A.1}$$

where the mapping function, g, is defined as

$$g(\zeta_v) = \zeta_v + \frac{R^2}{\zeta_v} \tag{A.2}$$

The derivative of z with respect to ζ_v is

$$\frac{dz_v}{d\zeta_v} = g'(\zeta_v)e^{i\alpha} \tag{A.3}$$

We also consider the case where the flat plate is moving with a constant speed U_∞, inclined to the x-axis by an angle α. A vortex of strength Γ_v is shed from the trailing edge as shown in Fig. 1. For this flow, the complex potential in the circle plane is written as [50,51,58]

$$\begin{aligned} F(\zeta_v) &= \phi(\zeta_v) + i\psi(\zeta_v) \\ &= V(\zeta_v - g(\zeta_v)) + \frac{R^2\bar{V}}{\zeta_v} \\ &\quad + \frac{\Gamma_v}{2\pi i}\left[\ln(\zeta_v - \zeta_v) - \ln(\zeta_v - \zeta_v^{(I)})\right] \end{aligned} \tag{A.4}$$

where ϕ is the velocity potential, ψ is the stream function, $V = -U_\infty e^{i\alpha}$ is the velocity of the flat plate in the plate-fixed frame, and $\zeta_v^I = R^2/\zeta_v^*$ denotes the position of the image vortex within the circle. The first term inside the brackets $(\zeta_v - g(\zeta_v))$ ensures that the complex potential will contain only ζ_v with negative power (see Sec. 9.63 [50], Sec. 4.71 [57], Sec. 4 [51], Sec. 3.2 [58]).

A.1. Dynamics of the starting vortex

Taking the origin at the mid-chord point and assuming that the starting vortex shed from the trailing edge ($\hat{z}_{v0} = -c/2$), we write the evolution equation of the starting vortex according to the Lagrangian dynamics as

$$\begin{aligned} \dot{z}_v + \frac{\dot{\Gamma}_v}{\beta\Gamma_v}(z_v - z_{v0}) &= (\frac{i}{\Gamma}\frac{\partial W}{\partial z_v})^* \\ &= (\frac{i}{\Gamma_v}\frac{\partial W}{\partial \zeta_v}(\frac{dz_v}{d\zeta_v})^{-1}_{z_v})^* \\ &= w^*(z_v) \end{aligned} \tag{A.5}$$

where β is a factor used to differentiate between the equation obtained from the proposed Lagrangian L $(\beta = 1)$ or Chapman's Lagrangian L' $(\beta = 2)$. Also, we have

$$W(z_v) = \Gamma_v \psi_o + \frac{\Gamma_v^2}{4\pi}|\ln(\zeta_v - \zeta_v^{(I)})| + \frac{\Gamma_v^2}{4\pi}\ln|\frac{dz}{d\zeta}|_{z_v} \tag{A.6}$$

and

$$\psi_0 = Im\left(V(\zeta_v - g(\zeta_v)) + \frac{R^2 V^*}{\zeta_v}\right) \tag{A.7}$$

Transforming Eq. (A.5) to the circle plane, the first term in the left hand side is written as

$$\dot{z}_v = U_\infty + g'(\zeta_v)e^{i\alpha}\dot{\zeta}_v \tag{A.8}$$

and the right hand side of Eq. (A.5) is re-written as

$$\begin{aligned} w^*(\zeta_v) &= \frac{e^{i\alpha}}{[g'(\zeta_v)]^*}\left[V(1 - g'(\zeta_v)) - \frac{R^2\bar{V}}{\zeta_v^2} - \frac{\Gamma_v}{2\pi i}\frac{1}{\zeta_v - \zeta_v^I}\right. \\ &\qquad \left. - \frac{\Gamma_v}{4\pi i}\frac{g''(\zeta_v)}{g'(\zeta_v)}\right]^* \\ &= \frac{e^{i\alpha}}{[g'(\zeta_v)]^*}\left[V - \frac{R^2\bar{V}}{\zeta_v^2} - \frac{\Gamma_v}{2\pi i}\frac{1}{\zeta_v - \zeta_v^I}\right. \\ &\qquad \left. - \frac{\Gamma_v}{4\pi i}\frac{g''(\zeta_v)}{g'(\zeta_v)}\right]^* - Ve^{-i\alpha} \end{aligned} \tag{A.9}$$

Recalling that $V = -U_\infty e^{i\alpha}$, we write

$$\begin{aligned} w^*(\zeta_v) &= \frac{e^{i\alpha}}{[g'(\zeta_v)]^*}\left[V - \frac{R^2\bar{V}}{\zeta_v^2} - \frac{\Gamma_v}{2\pi i}\frac{1}{\zeta_v - \zeta_v^I} - \frac{\Gamma_v}{4\pi i}\frac{g''(\zeta_v)}{g'(\zeta_v)}\right]^* \\ &\quad + U_\infty \end{aligned} \tag{A.10}$$

The evolution equation is then re-written in terms of the circle-plane variables as

$$\begin{aligned} &\dot{\zeta}_v + \frac{\dot{\Gamma}_v}{\beta\Gamma_v}\frac{(g(\zeta_v) - 2R)}{g'(\zeta_v)} \\ &= \frac{1}{g'(\zeta_v)[g'(\zeta_v)]^*}\left[V - \frac{R^2\bar{V}}{\zeta_v^2} - \frac{\Gamma}{2\pi i}\frac{1}{\zeta_v - \zeta_v^I} - \frac{\Gamma_v}{4\pi i}\frac{g''(\zeta_v)}{g'(\zeta_v)}\right]^* \end{aligned} \tag{A.11}$$

A more general form of Eq. (A.11), for $\beta = 1$, for a flat plate moving and rotating in space can be found in the work of Michelin and Smith [58], which will be used, without derivation, for the case of pitching flat plate.

A.2. Aerodynamic forces

The force on the flat plate is obtained using the force formula derived by Sedov [68], in terms of the complex variable z, as

$$F_x + iF_y = -i\rho z_o\frac{d\Gamma_v}{dt} + \overline{\frac{i\rho}{2}\int_C [w(z)]^2 dz} + \frac{d}{dt}\left[i\rho\int_C zw(z)dz\right] \tag{A.12}$$

Using Cauchy's theorem [69], the integration can be changed from an integration over the solid body C to an integration over the infinite domain C_∞ that excludes the integration over an infinitesimally small contour C_v around the vortex (see sec. 3.4.1 in Ref. [58]) as shown in Fig. A.7. Upon evaluating the integration, the force in terms of the complex variable ζ becomes

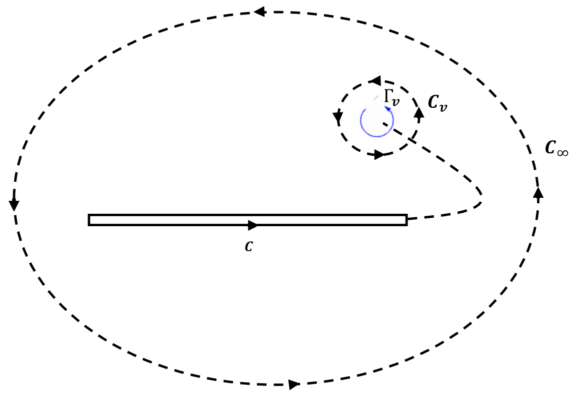

Fig. A.7. The contour used to evaluate the integral on the solid body. The flat plate is exaggerated to show the direction of the contour.

$$F_x + iF_y = i\rho e^{i\alpha}\left[2i\pi R^2 Im(V) + \frac{d}{dt}\left(\Gamma_v(\zeta_v - \frac{R^2}{\bar{\zeta}_v})\right)\right] \tag{A.13}$$

The vortex strength is calculated by satisfying the Kutta condition at each time instant. The Kutta condition is implemented by requiring that the tangential velocity at the trailing edge in the circle plane vanishes; i.e., the terms inside the brackets in Eq. (A.11) are set to zero at the trailing edge to cancel the singularity due to $1 - R^2/\zeta_{v0}^2 = 0$. This will ensure a finite velocity at the trailing edge. As such, we write

$$V - \frac{R^2\bar{V}}{\zeta_0^2} + \frac{\Gamma_v}{2\pi i}\left(\frac{1}{\zeta_0 - \zeta_v} - \frac{1}{\zeta_0 - \zeta_v^I}\right) = 0 \tag{A.14}$$

Equation (A.14) is then re-written as

$$2iIm(V) + \frac{\Gamma_v}{2\pi i}\left(\frac{-R^2 + (\eta_v + \xi_v)^2}{2(\eta_v^2 + (\xi_v - 2)^2)}\right) = 0 \tag{A.15}$$

where ξ_v and η_v are the real and imaginary parts of ζ_v.

By simple manipulation, Eq. (A.15) is re-written in a simple form as [58,48]

$$2Im(V) + \frac{\Gamma_v}{2\pi}Re\left(\frac{\zeta_{v0} + R}{\zeta_{v0} - R}\right) = 0 \tag{A.16}$$

For the force calculations using the impulse of the starting vortex, the reader is referred to section 3.10 of Ref. [24].

References

[1] L. Prandtl, Über die entstehung von wirbeln in der idealen flüssigkeit, mit anwendung auf die tragflügeltheorie und andere aufgaben, in: Vorträge aus dem Gebiete der Hydro- und Aerodynamik, Innsbruck, 1922, Springer, 1924, pp. 18–33.

[2] W. Birnbaum, Der schlagflugelpropeller und die kleinen schwingungen elastisch befestigter tragfluegel, Z. Flugtech. Mot.luftschiffahrt 15 (1924) 128–134.

[3] H. Wagner, Über die entstehung des dynamischen auftriebes von tragflügeln, ZAMM Z. Angew. Math. Mech. 5 (1) (1925) 17–35.

[4] T. Theodorsen, General Theory of Aerodynamic Instability and the Mechanism of Flutter, Tech. Rep. 496, NACA, 1935.

[5] J.G. Leishman, k.Q. Nguyen, State-space representation of unsteady airfoil behavior, AIAA J. 28 (5) (1990) 836–844.

[6] J.G. Leishman, G.L. Crouse, State-Space Model for Unsteady Airfoil Behavior and Dynamic Stall, no. 89-1319, AIAA, 1989, pp. 1372–1383.

[7] D.A. Peters, S. Karunamoorthy, W. Cao, Finite-state induced flow models, part I: two-dimensional thin airfoil, J. Aircr. 44 (1995) 1–28.

[8] D.A. Peters, Two-dimensional incompressible unsteady airfoil theory? An overview, J. Fluids Struct. 24 (3) (2008) 295–312.

[9] S.A. Ansari, R. Żbikowski, K. Knowles, Non-linear unsteady aerodynamic model for insect-like flapping wings in the hover. Part 1: methodology and analysis, Proc. Inst. Mech. Eng., G J. Aerosp. Eng. 220 (2) (2006) 61–83.

[10] S.A. Ansari, R. Zbikowski, K. Knowles, Non-linear unsteady aerodynamic model for insect-like flapping wings in the hover. Part 2: implementation and validation, J. Aerosp. Eng. 220 (2006) 169–186.

[11] H.E. Taha, M.R. Hajj, P.S. Beran, State space representation of the unsteady aerodynamics of flapping flight, Aerosp. Sci. Technol. 34 (2014) 1–11.
[12] Z. Yan, H.E. Taha, M.R. Hajj, Geometrically-exact unsteady model for airfoils undergoing large amplitude maneuvers, Aerosp. Sci. Technol. 39 (2014) 293–306.
[13] S. Belotserkovskii, Study of the unsteady aerodynamics of lifting surfaces using the computer, Annu. Rev. Fluid Mech. 9 (1) (1977) 469–494.
[14] C. Rehbach, Numerical calculation of three-dimensional unsteady flows with vortex sheets, in: 16th Aerospace Sciences Meeting, 1978, p. 111.
[15] E. Atta, O. Kandil, D. Mook, A. Nayfeh, Unsteady Aerodynamic Loads on Arbitrary Wings Including Wing-Tip and Leading-Edge Separation, AIAA paper 1977-0156, 1997.
[16] P. Konstadinopoulos, D. Thrasher, D. Mook, A. Nayfeh, L. Watson, A vortex-lattice method for general, unsteady aerodynamics, J. Aircr. 22 (1) (1985) 43–49.
[17] D. Levin, J. Katz, Vortex-lattice method for the calculation of the nonsteady separated flow over delta wings, J. Aircr. 18 (12) (1981) 1032–1037.
[18] J. Katz, Lateral aerodynamics of delta wings with leading-edge separation, AIAA J. 22 (3) (1984) 323–328.
[19] J. Katz, A. Plotkin, Low-Speed Aerodynamics, vol. 13, Cambridge University Press, 2001.
[20] G.-H. Cottet, P.D. Koumoutsakos, Vortex Methods: Theory and Practice, Cambridge University Press, 2000.
[21] K. Ramesh, A. Gopalarathnam, J.R. Edwards, M.V. Ol, K. Granlund, An unsteady airfoil theory applied to pitching motions validated against experiment and computation, Theor. Comput. Fluid Dyn. 27 (6) (2013) 843–864.
[22] K. Ramesh, A. Gopalarathnam, K. Granlund, M.V. Ol, J.R. Edwards, Discrete-vortex method with novel shedding criterion for unsteady aerofoil flows with intermittent leading-edge vortex shedding, J. Fluid Mech. 751 (2014) 500–538.
[23] H. Helmholtz, About integrals of hydrodynamic equations related with vortical motions, J. Reine Angew. Math. 55 (1858) 25.
[24] P.G. Saffman, Vortex Dynamics, Cambridge University Press, 1992.
[25] D. Darakananda, J. Eldredge, T. Colonius, D.R. Williams, A vortex sheet/point vortex dynamical model for unsteady separated flows, in: 54th AIAA Aerospace Sciences Meeting, AIAA SciTech, 2016, pp. 4–8.
[26] J. Li, Z.-N. Wu, A vortex force study for a flat plate at high angle of attack, J. Fluid Mech. 801 (2016) 222–249.
[27] X. He, I. Gursul, Point vortex model of deflected wakes of oscillating airfoils, AIAA J. 54 (11) (2016) 3647–3651.
[28] L. Cortelezzi, A. Leonard, Point vortex model of the unsteady separated flow past a semi-infinite plate with transverse motion, Fluid Dyn. Res. 11 (6) (1993) 263.
[29] A. Clebsch, Ueber die integration der hydrodynamischen gleichungen, J. Reine Angew. Math. 56 (1859) 1–10.
[30] G. Whitham, A general approach to linear and non-linear dispersive waves using a Lagrangian, J. Fluid Mech. 22 (02) (1965) 273–283.
[31] R. Hargreaves, XXXVII. A pressure-integral as kinetic potential, Philos. Mag. 16 (93) (1908) 436–444.
[32] H. Bateman, Notes on a differential equation which occurs in the two-dimensional motion of a compressible fluid and the associated variational problems, Proc. R. Soc. Lond., a Contain. Pap. Math. Phys. Character 125 (799) (1929) 598–618.
[33] J. Luke, A variational principle for a fluid with a free surface, J. Fluid Mech. 27 (02) (1967) 395–397.
[34] J. Serrin, Mathematical principles of classical fluid mechanics, in: Fluid Dynamics I/Strömungsmechanik I, Springer, 1959, pp. 125–263.
[35] M.I. Loffredo, Eulerian variational principle for ideal hydrodynamics and two-fluid representation, Phys. Lett. A 135 (4–5) (1989) 294–297.
[36] A. Rouhi, J. Wright, Hamiltonian formulation for the motion of vortices in the presence of a free surface for ideal flow, Phys. Rev. E 48 (3) (1993) 1850.
[37] E.F.G. Van Daalen, E. van Groesen, P.J. Zandbergen, A Hamiltonian formulation for nonlinear wave-body interactions, in: Eighth International Workshop on Water waves and Floating Bodies, IWWWFB, vol. 159163, 1993.
[38] D.M. Chapman, Ideal vortex motion in two dimensions: symmetries and conservation laws, J. Math. Phys. 19 (9) (1978) 1988–1992.
[39] B.N. Shashikanth, J.E. Marsden, J.W. Burdick, S.D. Kelly, The Hamiltonian structure of a two-dimensional rigid circular cylinder interacting dynamically with n point vortices, Phys. Fluids 14 (3) (2002) 1214–1227.
[40] L. Foeppl, Vortex Motion Behind a Circular Cylinder, NASA-TM-77015, 1983.
[41] A. Smith, On the stability of Foppl's vortices, J. Appl. Mech. 40 (2) (1973) 610–612.
[42] D.G. Dritschel, S. Boatto, The motion of point vortices on closed surfaces, Proc. R. Soc. A 471 (2015) 20140890.
[43] C.E. Brown, W.H. Michael, Effect of leading-edge separation on the lift of a delta wing, J. Aeronaut. Sci. 21 (1954) 690–695.
[44] R.H. Beckwith, H. Babinsky, Impulsively started flat plate flow, J. Aircr. 46 (6) (2009) 2186–2189.
[45] K. Granlund, M. Ol, D. Garmann, M. Visbal, L. Bernal, Experiments and Computations on Abstractions of Perching, AIAA paper 4943, 2010.
[46] C. Lin, On the motion of vortices in two dimensions-ii some further investigations on the Kirchhoff–Routh function, Proc. Natl. Acad. Sci. USA (1941) 575–577.
[47] R. Clements, An inviscid model of two-dimensional vortex shedding, J. Fluid Mech. 57 (02) (1973) 321–336.
[48] C. Wang, J.D. Eldredge, Low-order phenomenological modeling of leading-edge vortex formation, Theor. Comput. Fluid Dyn. 27 (5) (2013) 577–598.
[49] C. Lin, On the motion of vortices in two dimensions I. Existence of the Kirchhoff–Routh function, Proc. Natl. Acad. Sci. 27 (12) (1941) 570–575.
[50] L.M. Milne-Thompson, Theoretical Hydrodynamics, 5th ed., MacMillan, London, 1968, p. 1.
[51] E. Kanso, B.G. Oskouei, Stability of a coupled body-vortex system, J. Fluid Mech. 600 (2008) 77–94.
[52] H. Aref, Point vortex dynamics: a classical mathematics playground, J. Math. Phys. 48 (6) (2007) 065401.
[53] C.W. Rowley, J.E. Marsden, Variational integrators for degenerate Lagrangians, with application to point vortices, in: Proceedings of the 41st IEEE Conference on Decision and Control, 2002, vol. 2, IEEE, 2002, pp. 1521–1527.
[54] P.K. Newton, The N-Vortex Problem: Analytical Techniques, vol. 145, Springer Science & Business Media, 2013.
[55] D.T. Greenwood, Principles of Dynamics, Prentice-Hall, Englewood Cliffs, NJ, 1988.
[56] E.L. Hill, Hamilton's principle and the conservation theorems of mathematical physics, Rev. Mod. Phys. 23 (3) (1951) 253.
[57] H. Lamb, Hydrodynamics, Cambridge University Press, 1932.
[58] S. Michelin, S.G.L. Smith, An unsteady point vortex method for coupled fluid–solid problems, Theor. Comput. Fluid Dyn. 23 (2) (2009) 127–153.
[59] A.A. Tchieu, A. Leonard, A discrete-vortex model for the arbitrary motion of a thin airfoil with fluidic control, J. Fluids Struct. 27 (5) (2011) 680–693.
[60] S.A. Ragab, H.E. Fayed, Introduction to Finite Element Analysis for Engineers, CRC Press, 2017.
[61] T.V. Karman, Airfoil theory for non-uniform motion, J. Aeronaut. Sci. 5 (10) (1938) 379–390.
[62] J.D. Eldredge, Numerical simulation of the fluid dynamics of 2d rigid body motion with the vortex particle method, J. Comput. Phys. 221 (2) (2007) 626–648.
[63] H. Schlichting, et al., Boundary-Layer Theory, vol. 7, McGraw-Hill, New York, 1955.
[64] J. Eldredge, C. Wang, Improved Low-Order Modeling of a Pitching and Perching Plate, AIAA Paper 3579, 2011.
[65] D. Cleaver, Z. Wang, I. Gursul, Investigation of high-lift mechanisms for a flat-plate airfoil undergoing small-amplitude plunging oscillations, AIAA J. 51 (4) (2013) 968–980.
[66] D. Calderon, Z. Wang, I. Gursul, Lift-enhancing vortex flows generated by plunging rectangular wings with small amplitude, AIAA J. 51 (12) (2013) 2953–2964.
[67] Z. Sotoudeh, Y. Hwang, R.A. Canfield, A variational principle for unsteady compressible flow, in: 54th AIAA Aerospace Sciences Meeting, 2016, p. 1307.
[68] L.I. Sedov, Two-Dimensional Problems of Hydrodynamics and Aerodynamics, vol. 1, Nauka, Moscow, 1980.
[69] L.V. Ahlfors, Complex Analysis: An Introduction to the Theory of Analytic Functions of One Complex Variable, New York, London, 1953, p. 177.